Research Report

NO. 85-03

A BANDWIDTH EFFICIENT FREQUENCY-HOPPED
SPREAD SPECTRUM MODULATION STUDY

FINAL REPORT
PREPARED FOR THE DEPARTMENT OF COMMUNICATIONS
D.S.S. CONTRACT
OST84-00112

BY

P.H. WITTKE
P.J. McLANE
S.J. SIMMONS
Y.M. LAM

MARCH 1985

Queen's University at Kingston
Department of Electrical Engineering

A BANDWIDTH EFFICIENT FREQUENCY-HOPPED SPREAD SPECTRUM MODULATION STUDY

by

P.H. Wittke

P.J. McLane

S.J. Simmons

Y.M. Lam

Report No. 85-3

Final Report

Prepared for

The Department of Communications

Under DSS Contract No. OST84-00112

Department of Electrical Engineering

Queen's University

Kingston, Ontario, Canada

March, 1985

ABSTRACT

A study of piecewise coherent, frequency-hopped, spread spectrum signals and their reception is carried out. The modulation is assumed to be coherent in the interval between frequency hops. A number of modulation schemes in which the signal between hops is a bandwidth efficient, partial response encoded, digital FM modulation, are considered, as the data modulation band occupancy must be compact in order for systems with a slow-to-medium hopping rate to have reasonable processing gain. Power spectra are determined for hopping rates that are less than or equal to the symbol rate. A number of examples of spectra are plotted for hopped MSK, duobinary and tamed FM signals. Then the maximum likelihood sequence estimating receiver for reception over a single hop interval is presented, and it is shown how the receiver can be implemented by a practical recursive algorithm based on dynamic programming ideas. The example of MSK is considered in detail. Finally, the case of reception spanning frequency hops is considered.

1. INTRODUCTION

Under the Space Sector military program, the Communications Research Centre has from the Department of National Defence the task of the development of spread spectrum modulation. The goal is to provide an electronic counter-countermeasures capability to military satellite communications. Recently, the trend in MIL-SATCOM has been to communications at EHF and the use of fast frequency-hopped, M-ary FSK or DPSK based spread spectrum signal structures. There appears a need to examine the possible anti-jam protection of high data rate systems. In this situation, the bandwidth occupied by the dehopped, modulated signal is of prime importance and relates directly to the degree of protection achievable. Thus there appears a possible advantage in the use of a bandwidth efficient coherent frequency modulation scheme for the transmission of a number of bits during each hop interval. In particular, we will examine the broad class of band-efficient signals that can be generated or represented as a frequency modulation by a multi-level partial response signalling with pulse shaping. This includes MSK, tamed FM and DPSK. This report is on these signals, their power spectrum and their reception.

In working under previous contracts with the Space Systems Section of the Department of Communications, encoding [1], and signal-shaping techniques [2], for phase-continuous FSK were developed which gave improved spectral occupancy and error performance. Also new, less complicated receiver structures were

obtained [3-6].

In the present study the hopping rate is taken to be smaller than the rate of data transmission. Accordingly, processing gain is sacrificed to supply a multi-user service at both low and medium data rates. Since the processing gain is the ratio of the hopped bandwidth to the data bandwidth the precise computation of the latter is of considerable importance. In this study the power spectrum of frequency hopped, encoded digital frequency modulation (FM) is determined. The analysis holds for general hopping and data rates, and the modulated signal is taken to be phase coherent between frequency hops. In the latter part of the report the algorithm for noncoherent, maximum likelihood sequence detection is presented. This is for slow hopped, digital FM in an additive white Gaussian noise environment. Performance analysis should follow the earlier work in references [7, 8], when a hop-time does not occur in the data sequence for detection. The performance analysis of the more important case which involves a frequency hop during sequence detection is left for further study.

2. SIGNAL MODEL

In this section, we will present the signal under study. The signal is basically a hopped signal with a random hop occurring after every N transmitted symbols or every NT seconds. During any one hop interval, the modulation is assumed to be coherent frequency modulation, with correlative or partial response encoding and shaping of the modulating pulses permissible. The trans-

mitter is shown in Fig.1. Thus the modulated signal of interest is of the form

$$s(t) = \sum_{n=-\infty}^{\infty} p(t-iNT) \cos[\omega_i t + \int^{t} m(u)du + \theta_i] \qquad (1)$$

where $p(t) = 1 \qquad 0 \leq t \leq NT,$

$= 0 \qquad$ elsewhere,

ω_i is the frequency of the i^{th} hop,

θ_i is the initial phase at the start of the i^{th} hop, and

$m(t)$ is the correlatively encoded modulating signal.

With the usual model for correlative encoding [1], the transmitted message can be written in terms of correlated variables

$$m(t) = \sum_{n=-\infty}^{\infty} J_n g(t-nT) \qquad (2)$$

where the correlated variables J_n are expressed in terms of the input symbols by

$$J_n = \frac{1}{C} \sum_{j=0}^{m} k_j \, I_{n-j} \qquad (3)$$

with the normalisation $C = \sum_{j=0}^{m} |k_j|$. Alternatively, the modulating signal can be expressed as a modulation by overlapping pulses $b(t)$,

$$m(t) = \sum_{n=-\infty}^{\infty} I_n \, b(t-nT), \qquad (4)$$

where the overlapping pulses are given by

$$b(t) = \frac{1}{C} \sum_{i=0}^{m} k_i \, g(t-iT)$$

For M-ary transmission, the I_n are independent identically distributed random variables that can take on M discrete values.

3. THE SPECTRUM OF PIECEWISE COHERENT FREQUENCY HOPPED DIGITAL FM

In this section of the report we will derive an expression for the spectrum of our piecewise coherent M-ary FM signal which has been noncoherently hopped and then noncoherently dehopped. It is assumed that there is an intermediate frequency offset ω_c (which could be zero) between the hopping and the dehopping frequencies. As expected, the spectrum will appear related to the spectrum of the coherent signal and that of a signal hopped every NT seconds.

The modulated signal of interest is of the form

$$s(t) = \sum_{i=-\infty}^{\infty} p(t-iNT) \cos[\omega_c t + \int^t m(u)du + \theta_i] \qquad (5)$$

For M-ary transmission I_n can take on the values $\pm 1, \pm 3 .. \pm(M-1)$. The incoherent hopping results in statistically independent random initial phases θ_i, that are assumed to be uniformly distributed over $(0,2\pi)$.

The signal can be written in terms of a complex baseband equivalent

$$s(t) = \mathrm{Re}\{\rho(t)\exp[j\omega_c t]\}$$

where

$$\rho(t) = \sum_{i=-\infty}^{\infty} p(t-iNT)\exp j[\theta_i + \int^t \sum_{n=-\infty}^{\infty} I_n\, b(u-nT)\, du \qquad (6)$$

Here Re denotes the real part, and * as a superscript denotes the complex conjugate.

The autocorrelation function will be used to find the signal spectrum. Then

$$R(t,t+\tau) = (1/4)[E\{\rho(t)\rho(t+\tau)\}\exp j\omega_c(2t+\tau) + E\{\rho(t)\rho^*(t+\tau)\}\exp -j\omega_c\tau + E\{\rho^*(t)\rho(t+\tau)\}\exp j\omega_c\tau + E\{\rho^*(t)\rho^*(t+\tau)\}\exp -j\omega_c(2t+\tau)].$$

Due to the assumption of uniformly distributed θ_i, $E\{\rho(t)\rho(t+\tau)\}=0$, and the first and last terms in the expression for $R(t,t+\tau)$ vanish. Thus the autoccorrelation function

$$R(t,t+\tau) = (1/2)\mathrm{Re}\{E\{\rho^*(t)\rho(t+\tau)\}\exp j\omega_c\tau\} \tag{7}$$

The expectation in (7) is given by

$$E\{\rho^*(t)\rho(t+\tau)\} = \sum_{i=-\infty}^{\infty}\ \sum_{j=-\infty}^{\infty} p(t-iNT)p(t+\tau-jNT)\ \xi$$

where

$$\xi = E\{\exp j[\int_t^{t+\tau} m(u)\ du + \theta_i-\theta_j]\}$$

$$= E\{\exp j[\int_{t-iNT}^{t-iNT+\tau} m(u)\ du]\}\cdot\delta_{i,j} \tag{8}$$

In this last equation, use has been made of the cyclostationary nature of the modulating signal, in that there is no change in the expectation if the interval of integration is shifted by an integer number of bits. Here the shift is by iN bits or a duration of iNT.

The autocorrelation function

$$R(t,t+\tau) = (1/2)\mathrm{Re}\{E\{\rho^*(t)\rho(t+\tau)\}\exp j\omega_c\tau\}$$

is a function of t. In other words the signal s(t) is not wide-sense stationary but is in fact cyclostationary (see [13]), that is, $R(t+NT,t+\tau+NT) = R(t,t+\tau)$. This can be dealt with as follows.

Since in practice we do not have a precise time origin, we can

assume that the origin is uniformly distributed over (0,NT)

$$f_t(\eta) = (1/NT) \qquad 0 \leq \eta \leq NT$$
$$= 0 \qquad \text{elsewhere.}$$

The average autocorrelation function is

$$R(\tau) = E_t\{R(t,t+\tau)\}.$$

$$= (1/2)\mathrm{Re}[E_t\{E\{\rho^*(t)\rho(t+\tau)\}\}\exp j\omega_c\tau] \tag{9}$$

Now

$$E_t\{E\{\rho^*(t)\rho(t+\tau)\}\} = (1/NT)\int_0^{NT} E\{\rho^*(t)\rho(t+\tau)\}\,dt$$

$$= (1/NT)\sum_i \int_0^{NT} p(t-iNT)\,p(t+\tau-iNT)\,E\{\exp[j\int_{t-iNT}^{t+\tau-iNT} m(u)\,du]\}\,dt$$

$$= (1/NT)\int_{-\infty}^{\infty} p(t)\,p(t+\tau)\,E\{\exp[j\int_t^{t+\tau} m(u)\,du\}\,dt \tag{10}$$

Finally, if (10) is substituted in (9), there results

$$R(\tau) = (1/2NT)\int_{-\infty}^{\infty} p(t)\,p(t+\tau)\,R_{FM}(t,t+\tau)\,dt, \tag{11}$$

where R_{FM} is the autocorrelation function of the corresponding digital FM signal given by

$$R_{FM}(t,t+\tau) = E\{\cos(\omega_c\tau + \int_t^{t+\tau} m(u)\,du)\} \tag{12}$$

Bit Timing and Hopping Unsynchronized

Suppose that the hopping and bit timing are not synchronized. Then the results for the autocorrelation function and spectrum of the signal simplify dramatically. In this case, the initial time t, in (12) has a probability distribution over the interval (0,T) and the usual assumption of a uniform distribution will be made.

Then

$$R_{FM}(t\ t+\tau) = (1/T) \int_0^T E\{\cos(\omega_c \tau + \int_t^{t+\tau} m(u)\, du\}\, dt \qquad (13)$$

which is not a function of time and so will be denoted by $R_{FM}(\tau)$. It is the usual autocorrelation for digital FM. In this case (11) simplifies to give

$$R(\tau) = (1/2NT)[R_{FM}(\tau)\ R_p] \qquad (14)$$

where R_p is the autocorrelation of the hopping pulse defined by

$$R_p(\tau) = \int_{-\infty}^{\infty} p(t)p(t+\tau)dt \qquad (15)$$

The spectral density of the hopped signal simplifies to

$$S(\omega) = (1/2NT)[S_{FM}(\omega) * S_p(\omega)]$$

Here S_{FM} denotes the spectral density of the unhopped digital FM signal,

S_p denotes the spectral density of the hopping pulse, and

* denotes convolution.

Typical spectra are shown in Figs. 2 to 6. In each case the spectrum is plotted for a number of hop intervals NT, ranging from a hop every T secs., to the case of an infinite hop interval (or no hop at all). It is seen that as the hop interval is increased, the spectrum approaches that of the unhopped signal with the underlying digital FM modulation. This is as would be expected.

The following examples were chosen as typical.

(a) Fig. 2. Digital FM with a rectangular pulse and modulation index h=0.5. This is commonly referred to as MSK.

(b) Fig. 3. Duobinary FM, h=0.5 and rectangular pulse shaping.

(c) Fig. 4. Duobinary FM, h=0.7 and rectangular pulse shaping.

(d) Fig. 5. Partial response encoded FM, with polynomial $(1+D)^2/4$, h=0.5, and raised cosine frequency pulse shaping. This is commonly referred to as Tamed FM.

(e) Fig. 6. Partial response encoded FM, with polynomial $(1+D)^2/4$, h=0.7, and raised cosine frequency pulse shaping.

4. RECEIVER THEORY

4.1 Introduction

Up to this point the spectral analysis of a frequency-hopped system using digital FM has been considered. In this section, the maximum likelihood sequence estimation (MLSE) receiver algorithm is derived. We will assume noncoherent processing and a constant offset phase over the sequence length. Such an assumption pertains to the case where a frequency hop does not occur during the sequence under consideration. Taking account of the phase-jump that would occur at a frequency hop is non-trivial and is considered in Section 5.

Our derivation of the MLSE algorithm follows the tutorial paper by Hayes [9]. The algorithm we obtain is simpler than that proposed by Pawula and Golden [10], whose work involved the inclusion of coding. Early work on the performance of noncoherent receivers for digital FM is given in references [7] and [8]. All the relevant references for coherent MLSE algorithms are given in

Hayes' paper [9]. Our work herein closely follows the derivation of the algorithms presented in [5]; these algorithms are presented in more detail in [6,11]. There Thorpe considers a partially coherent MLSE receiver algorithm. The algorithm presented here is for the noncoherent case.

4.2 Sequence Detection Theory

The sequence detection problem to be solved can be stated as a hypothesis testing problem as follows: for $0 \leq t \leq NT$ decide which of the following M^N hypotheses holds

$$H_i: \quad r(t) = \sqrt{\frac{2E}{T}} \cos(2\pi f_c t + \psi_i(t) + \theta) + n(t)$$

$$i = 1,2,\ldots, M^N$$

where

$$\psi_i(t) = \pi h \sum_{n=0}^{N-1} J_{ni}\, g(t-nT)$$

and

$$g(t) = \int_{-\infty}^{t} p(\tau)d\tau$$

with J_n given by (3). Also if p(t) is of duration LT, g(LT) = 1 and thus h is the modulation index. Finally, for the class of signals we consider E is the signal energy, T is the symbol interval, θ is a constant, but random, phase offset and N is the length of the sequence of data symbols for sequence estimation. In our detection problem n(t) is white Gaussian noise with a spectral height of $N_o/2$ W/Hz.

The decision variable for the detection problem at hand can easily be shown to be [12, p.337]

$$\ell_i = E_\theta\{\exp[\frac{2}{N_o}\int_o^{NT} r(t)s(t, A_i, \theta)dt]\} \tag{16}$$

where $1 \leq i \leq M^N$,

$$s(t, A_i, \theta) = \sqrt{\frac{2E}{T}}\cos(2\pi f_c t + \psi_i(t) + \theta) \tag{16a}$$

$$A_i = \{I_{0,i}, I_{1,i}, \ldots, I_{N-1,i}\} \tag{16b}$$

and $E_\theta\{\cdot\}$ denotes mathematical expectation with respect to the random variable θ. The N-tuple A_i is the i-th possible sequence of the sequence being estimated. It is crucial to note that in sequence detection the N-tuple A_i is fixed for the i-th possible signal in the hypothesis detection problem stated above. This leads to a simpler estimation algorithm than would occur for optimization using bit-by-bit detection.

The remark we have just made leads to considerable simplification relative to the noncoherent receiver algorithms considered in [7,8,10]. To proceed expand the cosine function in (16a) (with respect to θ) using standard trigonometric identities to give for ℓ_i in (16):

$$\ell_i = E_\theta\{\exp\{\frac{2a}{N_o}[\ \ell_{cNi}^2 + \ell_{sNi}^2\ ]^{1/2}\cdot\cos(\theta + {}_i\lambda\ )\}\} \tag{17}$$

where

$$\ell_{cNi} = \int_o^{NT} r(t)\cos[2\pi f_c t + \psi_i(t)]dt \tag{18}$$

$$\ell_{sNi} = \int_o^{NT} r(t)\sin[2\pi f_c t + \psi_i(t)]dt \tag{19}$$

$$\lambda_i = \tan^{-1} \frac{\ell_{sNi}}{\ell_{cNi}}$$

and $a = \sqrt{2E/T}$. Now let θ be uniform in $[0, 2\pi]$. The expectation in (17) has occurred many times in detection theory for the random phase channel (see [12, p.339]). We have

$$\ell_i = I_o[\frac{2a}{N_o} (\ell_{cNi}^2 + \ell_{sNi}^2)^{1/2}] \tag{20}$$

where $I_o(x)$ is the modified Bessel function of order zero.

The solution to the detection problem at hand is to substitute each N-tuple in (16b) into the right-hand-side of (20) and choose the index i that renders ℓ_i a maximum. Fortunately the $I_o(\cdot)$ operation can be dispensed with as $I_o(x)$ is a monotone increasing function. Thus an equivalent decision variable is

$$\ell_i' = \ell_{cNi}^2 + \ell_{sNi}^2 \tag{21}$$

and in the next sub-section the detection algorithm is simplified.

4.3 The Dynamic Programming Algorithm

Of course the sequence of substitutions just described is too complex to be practical. As occurs in coherent systems, the optimization problem of maximizing ℓ_i' can be done in an efficient, sequential manner using Bellman's Dymanic Programming.

To proceed note that ℓ_{cNi} and ℓ_{sNi} in (18) and (19) respectively, can be computed using the following difference equation. For, $k = 0, 1, \ldots, N-1$,

$$\ell_{c,k+1,i} = \ell_{c,k,i} + \int_{kT}^{(k+1)T} r(t)\cos[2\pi f_c t + \psi_i(t)]dt \qquad (22)$$

$$\ell_{c,o,i} = 0 \qquad \ell_{cNi} = \ell_{c,k+1,i}$$

for k = N - 1.

Similarly, for ℓ_{sNi}

$$\ell_{s,k+1,i} = \ell_{s,k,i} + \int_{kT}^{(k+1)T} r(t)\sin(2\pi f_c t + \psi_i(t))dt \qquad (23)$$

$$\ell_{s,o,i} = 0 \qquad \ell_{sNi} = \ell_{s,k+1,i}$$

for k = N - 1.

At any stage k in the recursion

$$\ell_k' = \ell_{cki}^2 + \ell_{ski}^2 \qquad (24)$$

Furthermore,

$$\ell_k' = (\ell_{c,k-1,i} + \delta\ell_{cki})^2 + (\ell_{s,k-1\ i} + \delta\ell_{ski})^2 \qquad (25)$$

where $\delta\ell_{cki}$ and $\delta\ell_{ski}$ represent the second terms in equations (22) and (23) respectively. Note from (24) and (25) that ℓ_k', the metric, cannot be written in sequential form. However, it can be computed from the old information ($\ell_{c,k-1,i}$, $\ell_{s,k-1\ i}$) and the new information ($\delta\ell_{cki}$, $\delta\ell_{ski}$) in the k-th symbol interval.

The application of Bellman's Dynamic Programming in equation (25) yields the following functional equation that must be solved to determine the optimal estimate of the received data sequence:

$$\ell_k'^{*} = \max_{s_{k-1} \to s_k} \{(\ell_{c,k-1,i}^{*} + \delta\ell_{cki})^2 + (\ell_{s,k-1,i}^{*} + \delta\ell_{ski})^2\}$$

where the asterisk represents the optimal value of ℓ_k' and the maximum is computed over all states s_{k-1} that communicate with s_k.

Note that instead of storing the best metric for state s_{k-1} we must instead store the best pair $(\ell^*_{c,k-1,i}, \ell^*_{s,k-1,i})$ for state s_{k-1}. This leads to an increased storage requirement over that for the perfectly coherent case (see [5]). An increased storage requirement also occured in the partially coherent case treated by Thorpe [6].

4.4 The Example of MSK

Minimum-Shift-Keying is the simplest of the signals in the class of band-efficient digital FM signals. It occurs when h = 1/2 and the modulator pulse shape, p(t), is rectangular and of length T. We show the state diagram for MSK in Fig. 7 and its phase tree in Fig. 8. The state variables are the numbers 1 through 4 as shown in Fig. 7. During any bit interval the phase either increases or decreases by $\pi/2$ radians, the phase trajectory being a ramp function of slope $\pm\pi/2T$ radians per sec. The trellis diagram is shown in Fig. 9. Also shown are the Type A and Type B transitions, as only two states can be reached in any bit interval.

The computation of the metrics are produced by the structure shown in Fig. 10. For instance, ℓ_{c+} is the value of $\delta\ell_c$ when the expected signal has an increasing phase. With this information the metrics for the Type A transitions are shown in Fig. 11. Those for Type B transitions are shown in Fig. 12. For instance for Type A transitions into state 2 one computes

$$(\ell_{c1} + \ell_{c+})^2 + (\ell_{s1} + \ell_{s+})^2$$

and

$$(\ell_{c3} - \ell_{c-})^2 + (\ell_{s3} - \ell_{s-})^2$$

and chooses the largest. If the maximum occurs for the $1 \rightarrow 2$ transition we update (ℓ_{c1}, ℓ_{s1}) as follows:

$$\ell_{c2} \leftarrow \ell_{c1} + \ell_{c+}$$

$$\ell_{s2} \leftarrow \ell_{s1} + \ell_{s+}$$

The other state transitions in Figs. 11 and 12 are handled in an exactly analogous manner.

Note that sixteen quantities must be stored every two-bit intervals and also 8 squaring operations must be performed in the same period. In the coherent case, no squaring operation is involved and only four quantities are required for storage.

The MLSE algorithm for any other CPM signal can be derived by following the development for the case of MSK signalling. In future work the error event probabilities will be determined which will produce upper and lower bounds to the bit-error-probability. The calculations will be similar to that given in references [7] and [8]. Also the important problem of coping with a discontinuous phase shift that would occur at frequency hop times must be addressed. This is considered in the next section of the report.

5. PERIODICALLY DISCONTINUOUS PHASE JUMPS

5.1 Introduction

We now extend the theory in section 2 to include the case of a number of discontinuous phase jumps occurring over the period of the sequence detection. The receiver algorithm is relatively complex. However a special case of the algorithm can be combined with the algorithm of section 4 to produce a simple algorithm for a highly practical situation. This situation is the case of slow hopping where the hop rate is many times smaller than the data rate.

5.2 M Phase Jumps per N bit Intervals

The model to be used is shown in Fig. 13. A sequence length of NT seconds is displayed that contains M phase jumps or phase discontinuities. These are the points in time where a frequency hop occurs. In the time interval $0 < t < NT$ there are $K = N/M$ time intervals where the offset phase, θ_i, is constant; it is constant over a time interval of length MT. Each θ_i is uniform in $[0, 2\pi]$ and all θ_i are mutually independent.

Let $\underline{\theta}$ be the K-tuple, $(\theta_1, \theta_2, \ldots, \theta_K)$. Then the likelihood function in (16) becomes

$$\ell_i = E_{\underline{\theta}}\{\exp[\frac{2}{N_o}\int_o^{NT} r(t)s(t, A_i, \underline{\theta})dt]\} \qquad (26)$$

where

$$s(t, A_i, \underline{\theta}) = s(t, A_i, \theta_j)$$

for $(j-1)MT \leq t \leq jMT$ when $j = 1, \ldots, K = N/M$. As the θ_j are mutually independent

$$\ell_i = \prod_{j=1}^{K} E_{\theta_j} \{\frac{2}{N_o} \int_{(j-1)MT}^{jMT} r(t)s(t, A_i, \theta_j)dt\} \tag{27}$$

If we repeat the manipulations in going from equation (17) to (20) in equation (27) we get the following result:

$$\ell_i = \prod_{j=1}^{K} I_o \{\frac{2a}{N_o} \sqrt{\ell_{cji}^2 + \ell_{sj\ell}^2}\} \tag{28}$$

where, analogous to equations (17) and (28),

$$\ell_{cji} = \int_{(j-1)MT}^{jMT} r(t)\cos[2\pi f_c t + \psi_i(t)]dt \tag{29}$$

and

$$\ell_{sji} = \int_{(j-1)MT}^{jMT} r(t)\sin[2\pi f_c t + \psi_i(t)]dt \tag{30}$$

The subscript "j" now denotes that the correlations in (29) and (30) are computed over the j-th interval of constant phase shown in Fig.13. Note that for K = 1, i.e., only one interval of constant phase, the result in (28) reduces to our earlier result in (20).

Recall that one must compute ℓ_i for all M^N values of the sequence A_i in equation (16b). The computation in (28) can be done in a serial manner which leads to considerably less complexity. It is instructive to consider the case when K = N/M = 2.

First let $0 \leq t \leq MT$. Our algorithm operates exactly as in

Section 4. At time MT we have found the best pair (ℓ_{c1i}, ℓ_{s1i}) for each state variable in the trellis (see Fig. 9 for a trellis for the example of MSK). At time MT one computes

$$I_o \{\frac{2a}{N_o} \sqrt{\ell_{c1i}^2 + \ell_{s1i}^2}\}$$

for each state in the trellis at time MT.

The interesting point is what happens at the next time step. To illustrate this event, consider the state transition from states 1 and 3 into state 2 for the A-type transitions for MSK as shown in Fig.11. The state transitions under consideration are displayed in Fig.14. The first values of the new correlations (ℓ_{c2i}, ℓ_{s2i}) are found from the structure in Fig.10. Let the value of

$$I_o (\frac{2a}{N_o} [\ \ell_{c1i}^2 + \ell_{s1i}^2\ ]^{1/2})$$

at time MT for state ℓ be $I_o(\ell)$ where, in our example, $\ell = 1$ or 3 and $a = (2E/T)^{1/2}$. The comparison for the state transition 1 or 3 $\rightarrow$ 2 is

$$I_o(1)I_o(\frac{2a}{N_o} [\ \ell_{c+}^2 + \ell_{s+}^2\ ]^{1/2}) \qquad (31)$$

$$\text{vs} \quad I_o(2)I_o(\frac{2a}{N_o} [\ \ell_{c-}^2 + \ell_{s-}^2\ ]^{1/2})$$

Note that the modified Bessel functions must now be retained as a product of such functions is needed for the metric computations. The computations of (ℓ_{c2i}, ℓ_{s2i}) proceed serially as for the case when $j = 1$. Note also that the value of N_o is required which was not the case in section 2. The sequential detection algorithm has been described and the MSK example provided for $N/M = K = 2$.

However, the reader can easily generalize the algorithm for K > 2.

5.3 Simplification: M > > L.

Let the pulse length L of the frequency pulse for FM modulation be much less then M, where MT is the time interval over which the offset phase is constant. As such merges in the modulation trellis will occur much earlier than in M time intervals. This is illustrated in Fig. 15 for case of MSK (refer to Fig. 7 for the definition of state variables). Note that once the merge shown in Fig. 15 occurs, the factor $I_o(1)$ occurs in both comparisons in (31). Thus this factor can be dropped and the algorithm reverts back to that discussed in section 2.

Note that the more complicated comparisons like that in (31), which involve a table look up algorithm for the required Bessel functions, are required for only a few symbol intervals after the frequency hop. The number of such intervals as a multiple of the pulse length L would have to be determined by experiment. In any case for the case of slow hopping, i.e., M > > L, the MLSE detection algorithm can be simplified relative to the general case.

6. CONCLUDING REMARKS

A derivation of the power spectrum of piecewise coherent, frequency hopped, digital FM has been presented. Computations of the spectrum have been included for a number of bandwidth efficient, encoded, FM signals. A general maximum likelihood sequence

estimation algorithm has been presented for a dehopped, digital FM signal. This algorithm can be simplified when the hopping rate is much smaller than the data rate. Future work will concentrate on spectral calculations when the hop time is synchronous with a multiple of the bit time and on the performance analysis of the MLSE algorithm presented in this report.

REFERENCES

1. G.S. Deshpande and P.H. Wittke, "Correlative Encoded Digital FM", IEEE Trans on Comm., Vol. COM 29, pp. 156-162, February 1981.
2. G.S. Deshpande and P.H. Wittke, "Optimum Pulse Shaping in Digital Angle Modulation", IEEE Trans. on Comm., Vol. COM-29, pp. 162-168, February 1981.
3. S.J. Simmons and P.H. Wittke, "Low Complexity Decoders for Constant Envelope Digital Modulation", IEEE Trans. on Comm., Vol. COM-31, pp. 1273-1280, December, 1983.
4. S.J. Simmons and P.J. McLane, "Low Complexity Phase Tracking Decoders for Continuous Phase Modulation", Proc. IEEE Int. Conf. on Comm. Amsterdam, May 1984, pp. 924-929, to appear IEEE Trans. on Commun.
5. P.J. McLane, "The Viterbi Receiver for Correlative Encoded MSK Signals", IEEE Trans. on Comm., Vol. COM-31, pp. 290-295, February 1983.
6. J.B. Thorpe and P.J. Mclane, "A Hybrid Phase/Data Viterbi Demodux lator for Encoded CPFSK Modulation", Proc. Globecom '83, San Diego, Calif., Nov. 1983; to appear IEEE Trans. on Comm.

7. W.P. Osborne and M.B. Luntz, "Coherent and Noncoherent Detection of CPFSK", IEEE Trans. on Comm., Vol. COM-22, pp. 1023-1036, August 1974.

8. T.A. Schonhoff, "Symbol Error Probabilities for M-Ary CPFSK: Coherent and Noncoherent Detection", IEEE Trans. on Comm., Vol. COM-24, pp. 644-652, June 1976.

9. J.F. Hayes, "The Viterbi Algorithm Applied to Digital Data Transmission", Communications Society Magazine, Vol. 13, pp. 15-20, March 1975.

10. R.F. Pawula and R. Golden, "Simulation of Convolutional Coding/Viterbi Decoding with Noncoherent CPFSK", IEEE Trans. on Comm., Vol. COM-29, pp. 1522-1526, October 1981.

11. J.B. Thorpe, "A Finite Metric Hybrid Phase/Data Demodulator for Encoded CPFSK Modulation", M.Sc. Thesis, Queen's University, October 1983.

12. H.L. Van Trees, "Detection, Estimation, and Linear Modulation Theory, Part I", John Wiley and Sons, New York, 1968.

13. L.E. Franks, Signal Theory, Prentice-Hall Inc., 1969.

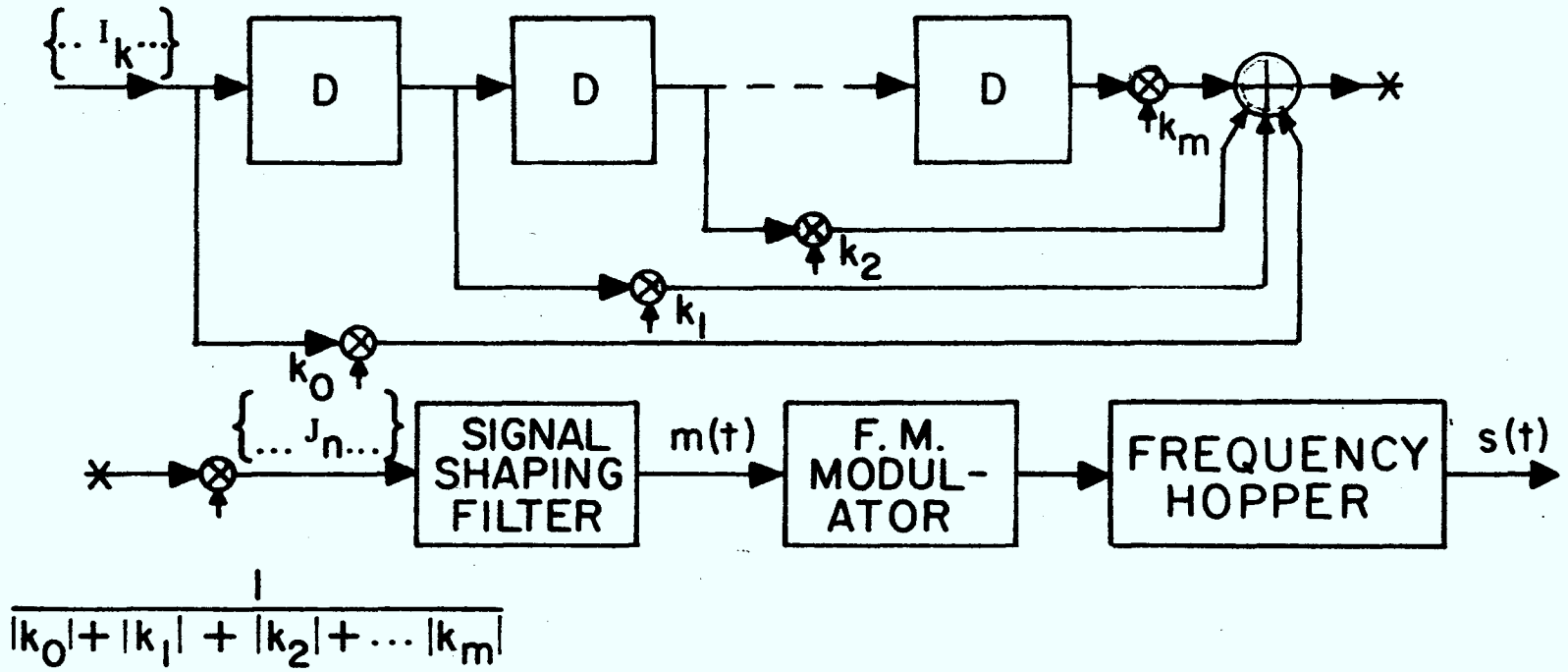

Fig. 1. Bandwidth Efficient Frequency-hopped Transmitter.

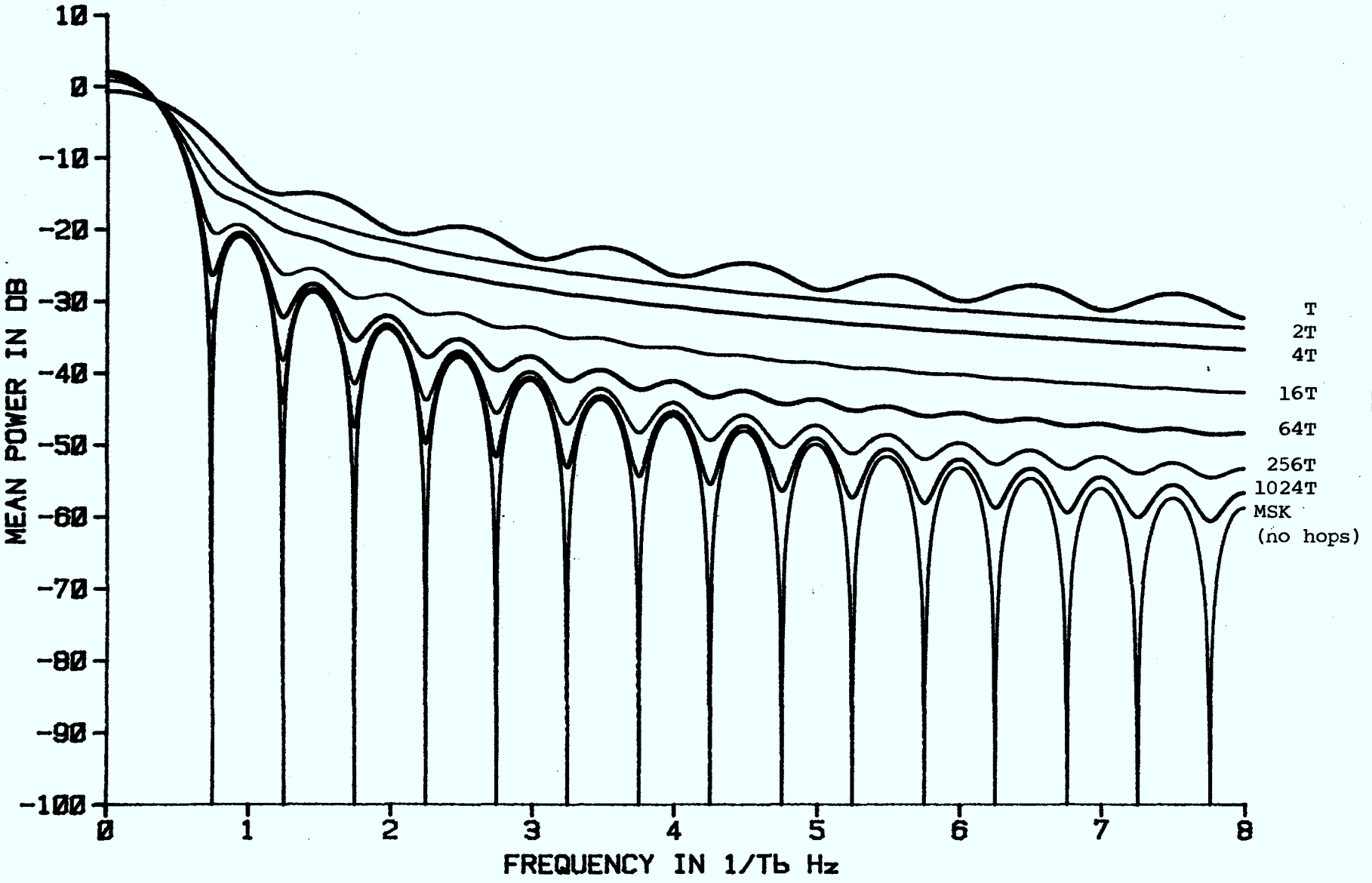

Fig. 2 Hopped MSK

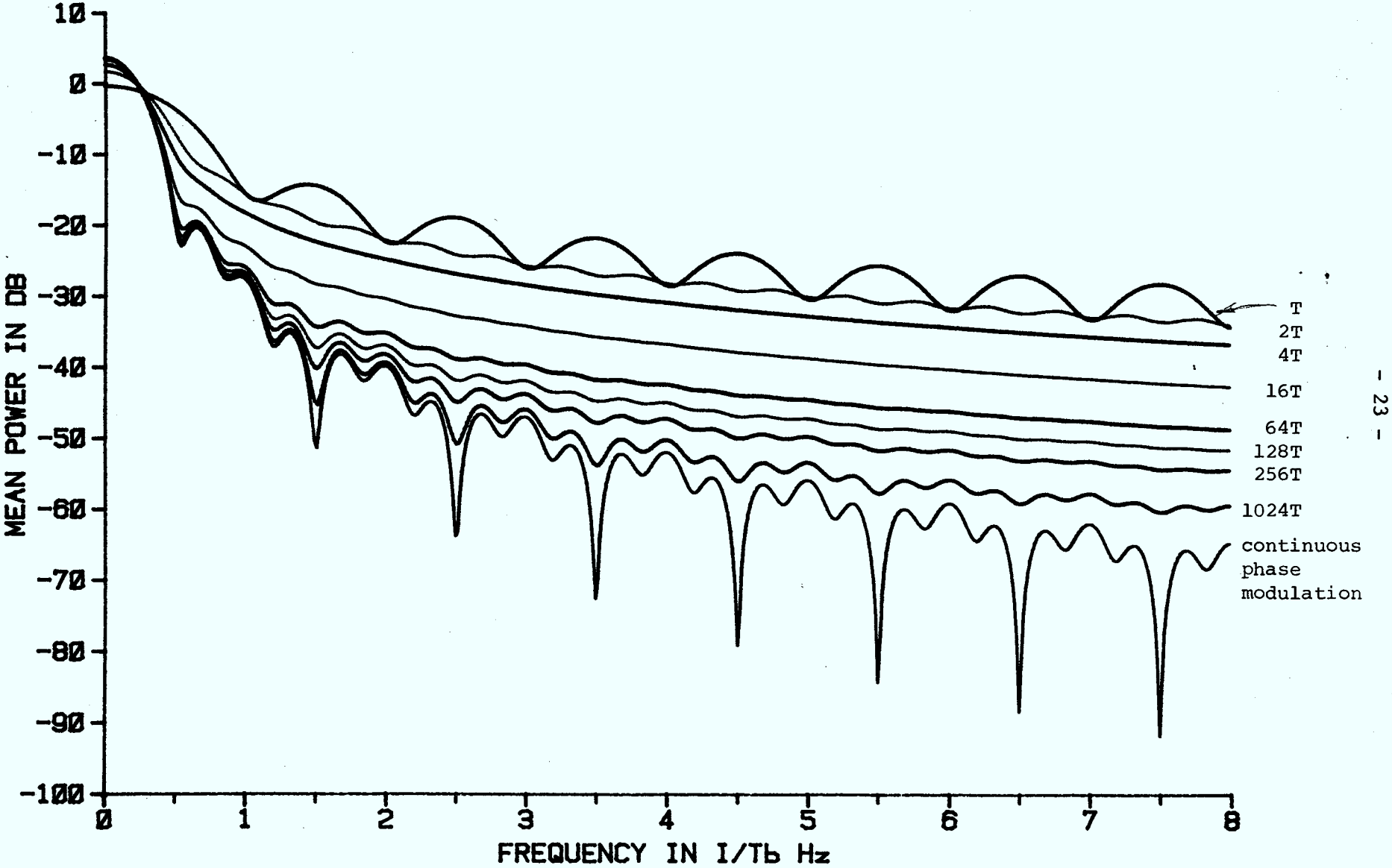

Fig. 3 Hopped Duobinary FSK, h=0.5

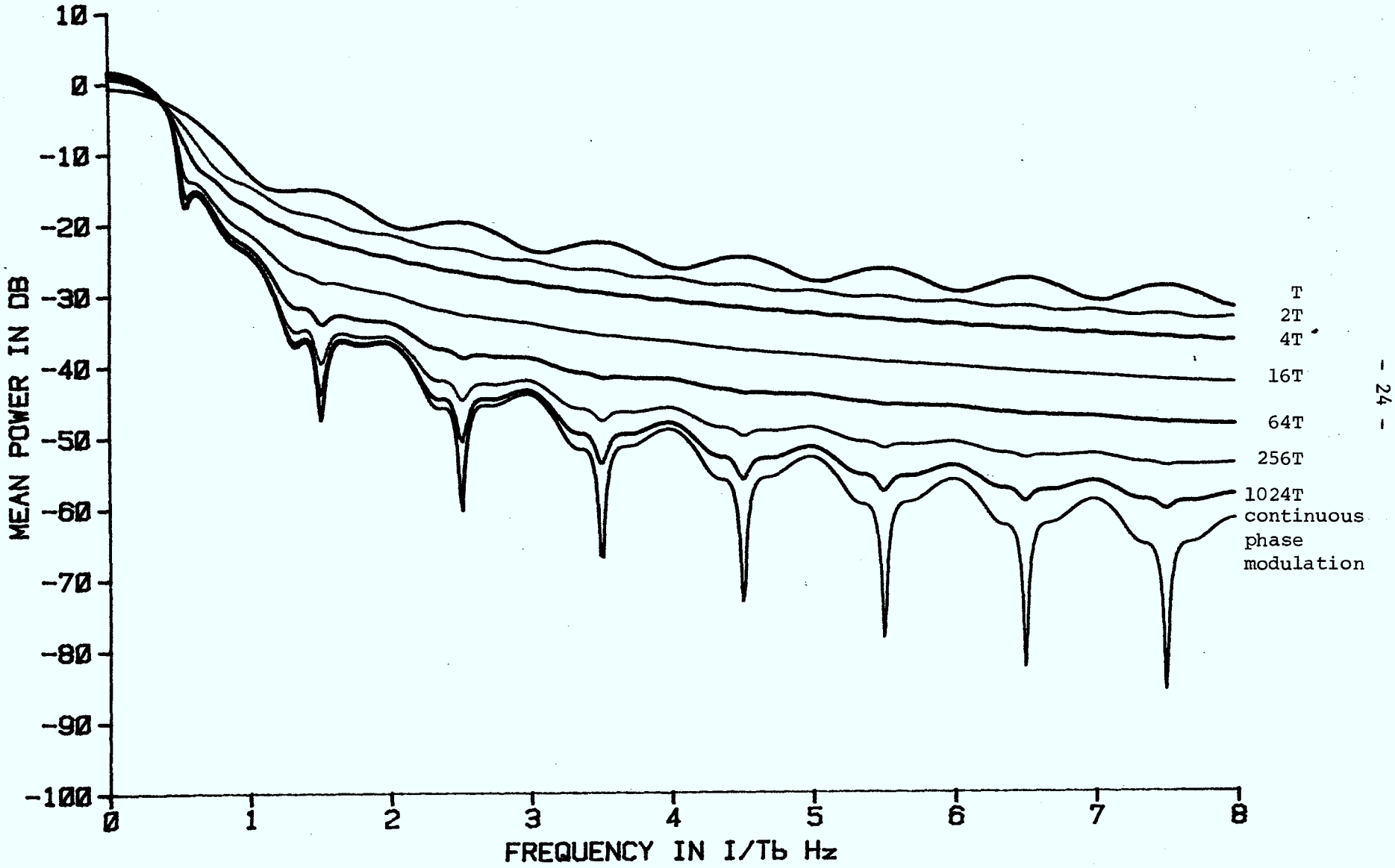

Fig. 4 Hopped Duobinary FSK, h=0.7

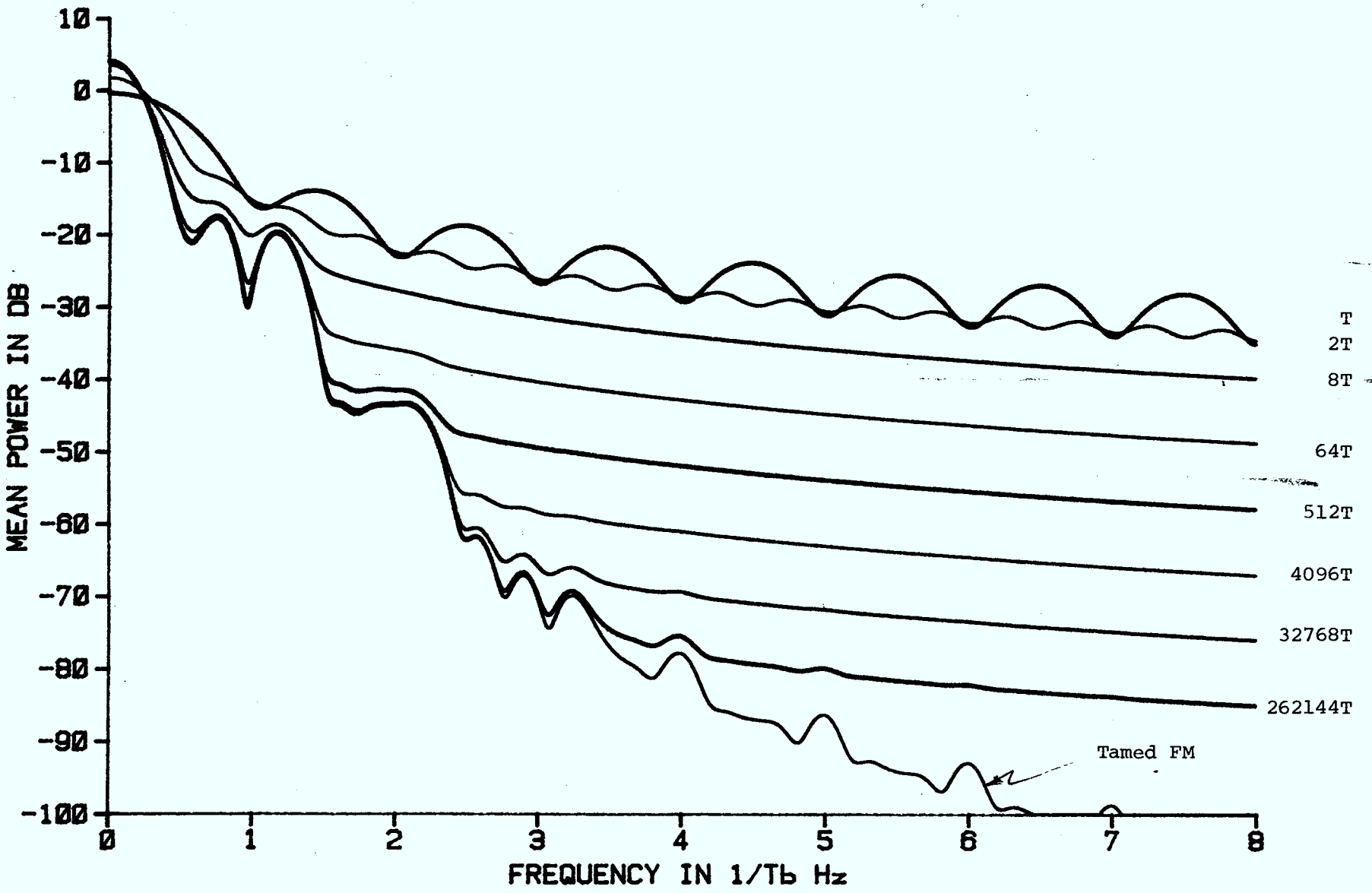

Fig. 5 Hopped Tamed FM, h=0.5

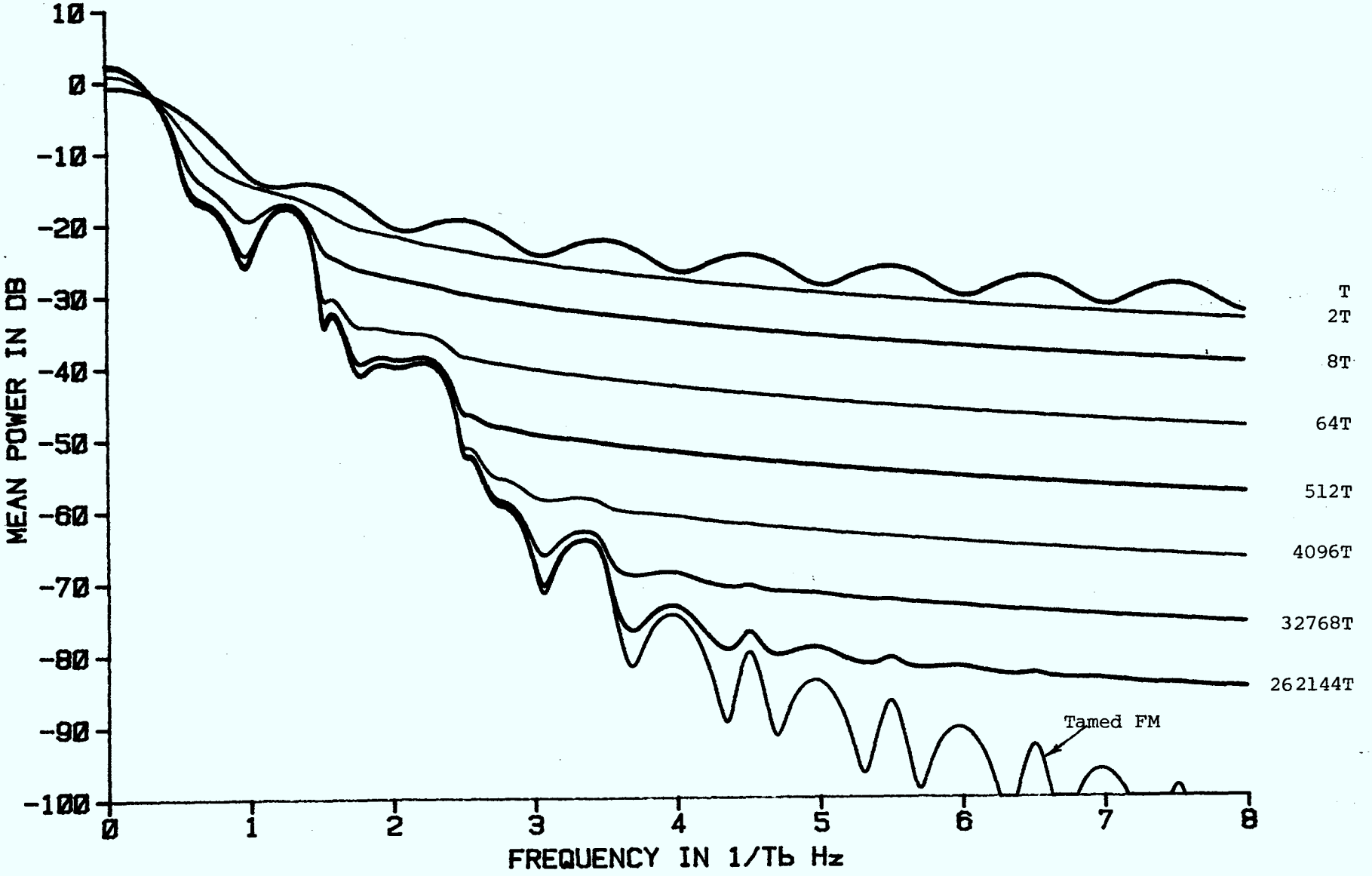

Fig. 6 Hopped Tamed FM, h=0.7

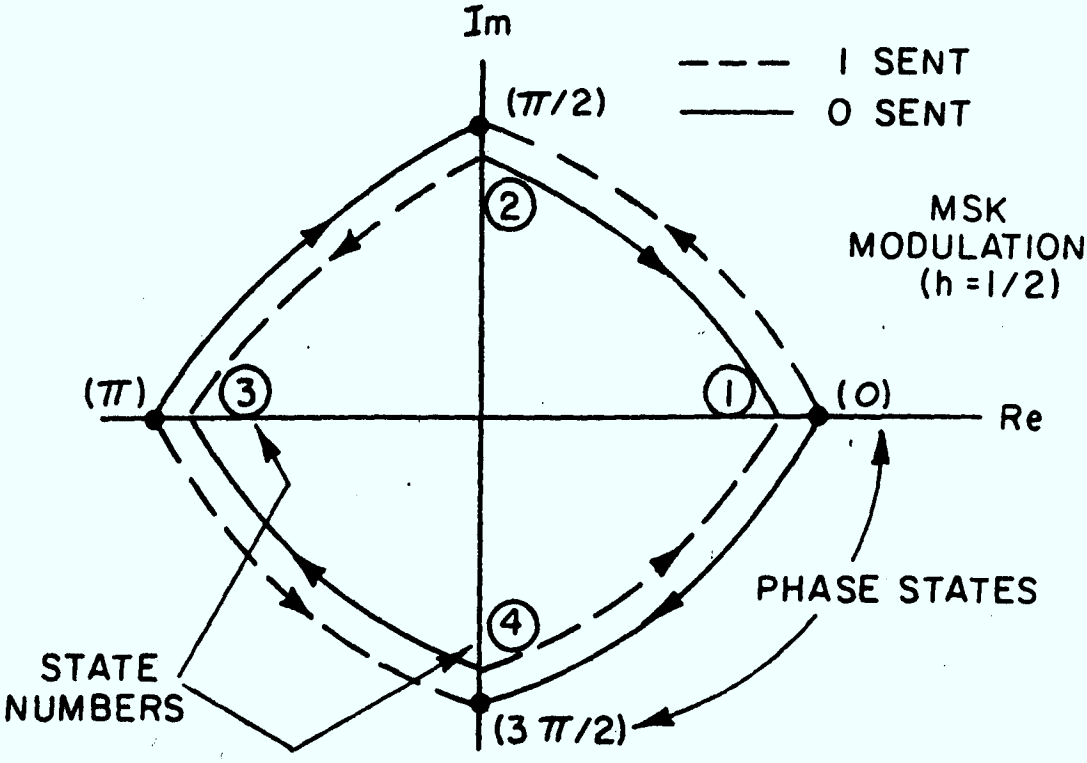

Figure 7 Phasor state diagram for MSK modulation

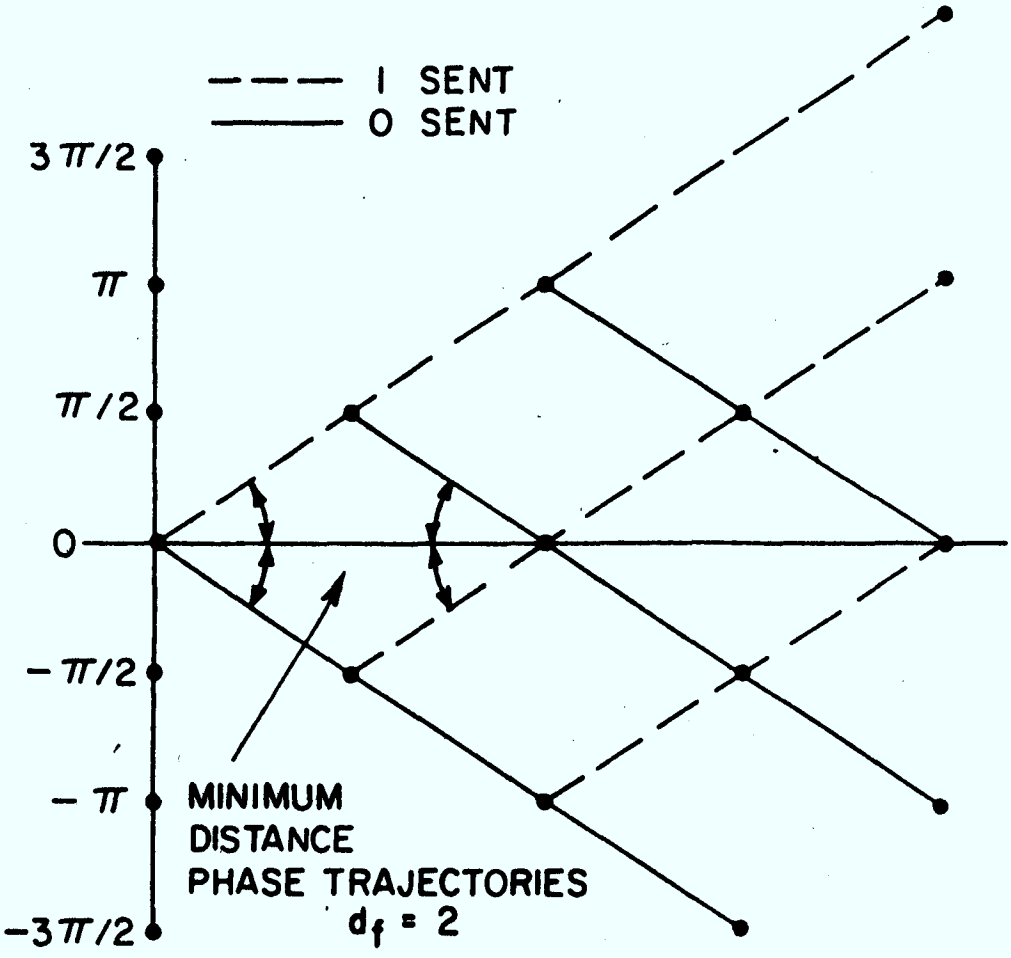

Figure 8 Phase tree for MSK modulation

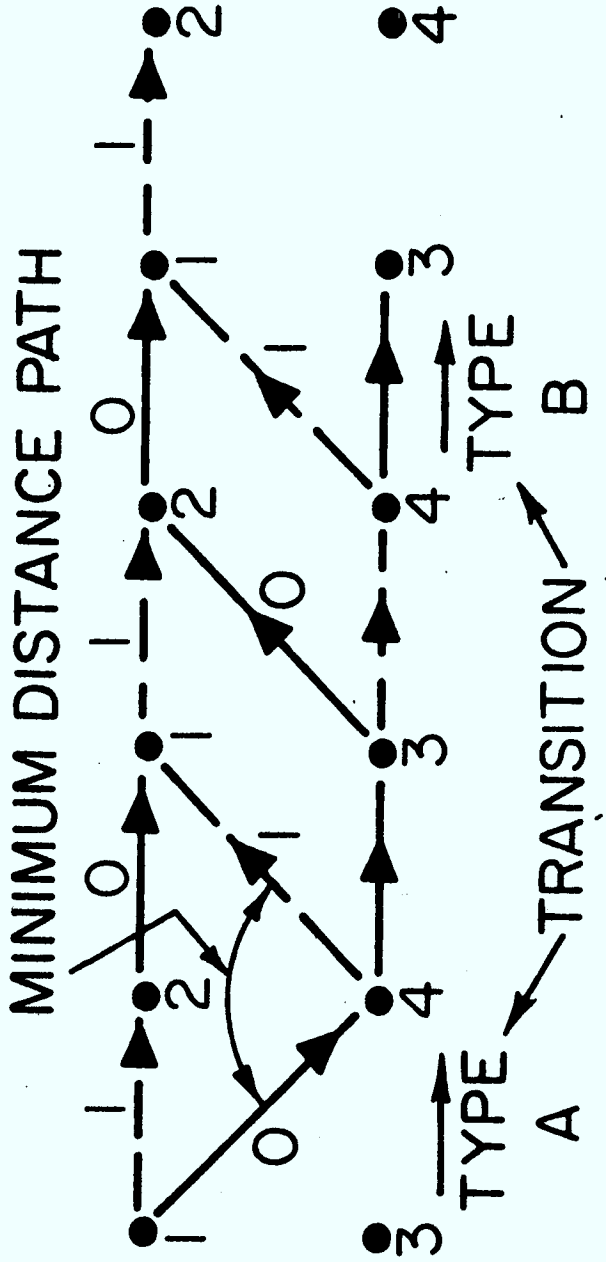

Figure 9 Trellis for MSK demodulation using the Viterbi detector

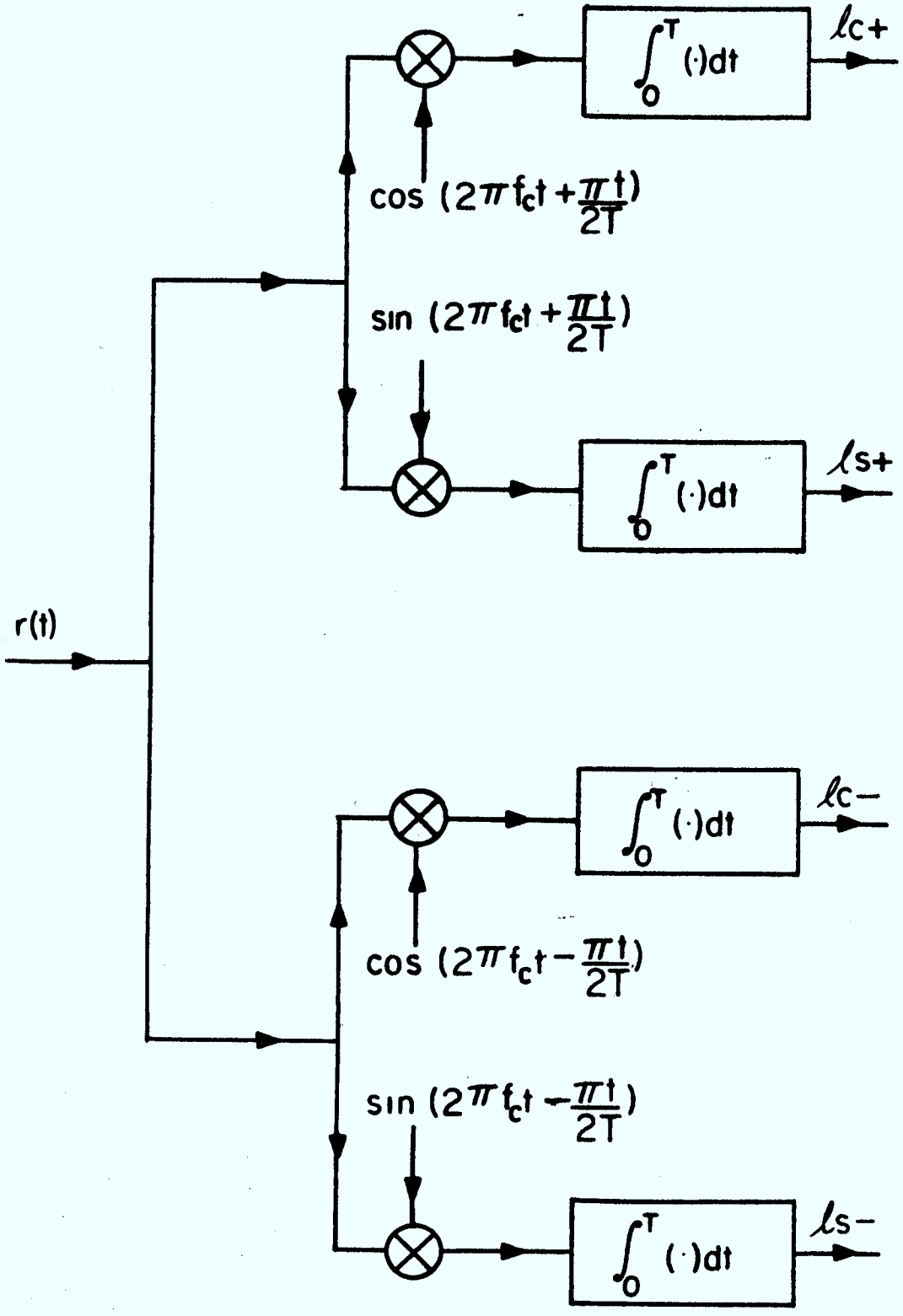

Figure 10 Metrics for coherent or noncoherent maximum likelihood sequence estimation for MSK.

TABLE TYPE A TRANSITIONS

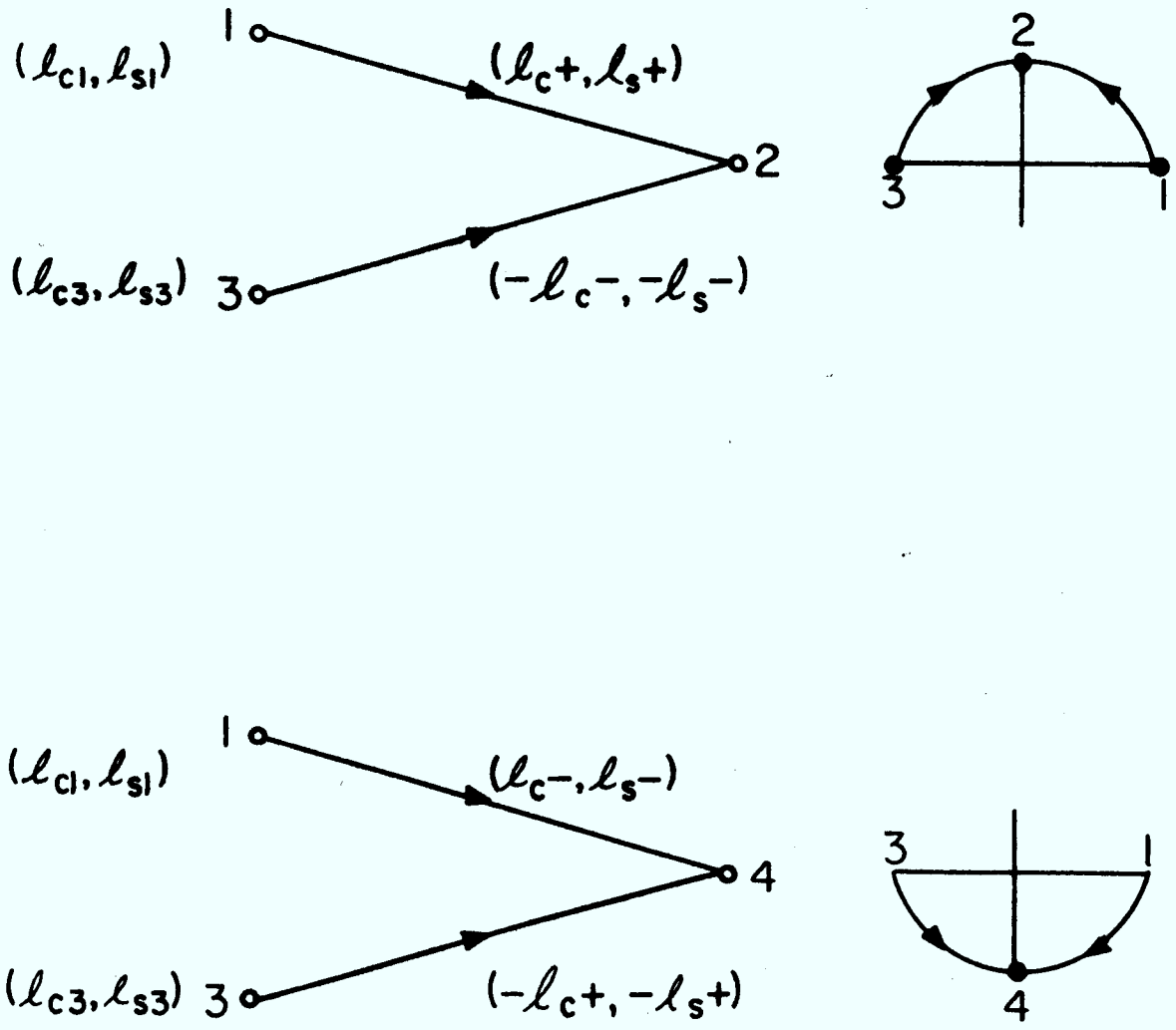

Figure 11 Path metrics for type A transitions for MSK.

TABLE TYPE B TRANSITIONS

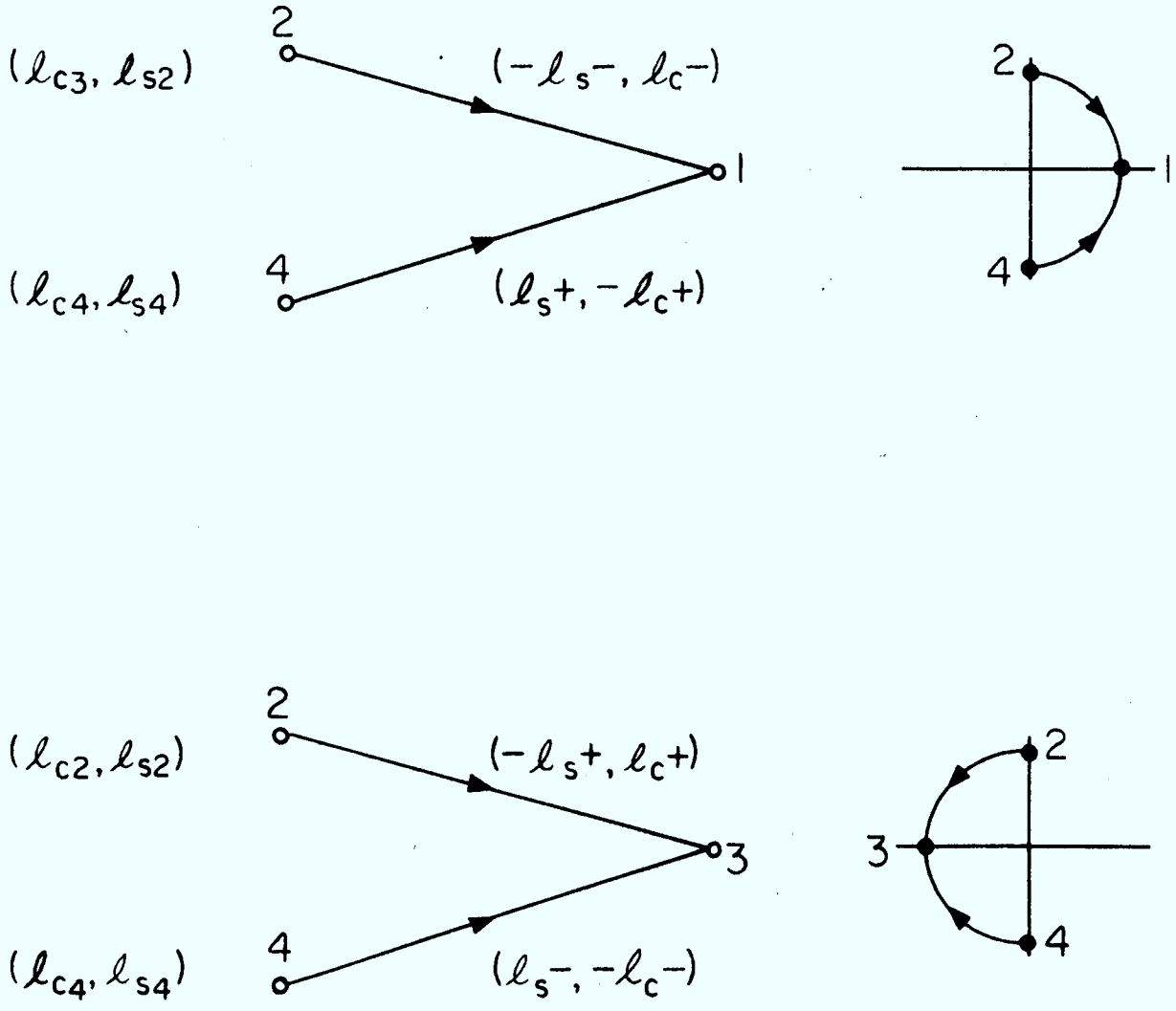

Figure 12 Path metrics for type B transitions for MSK.

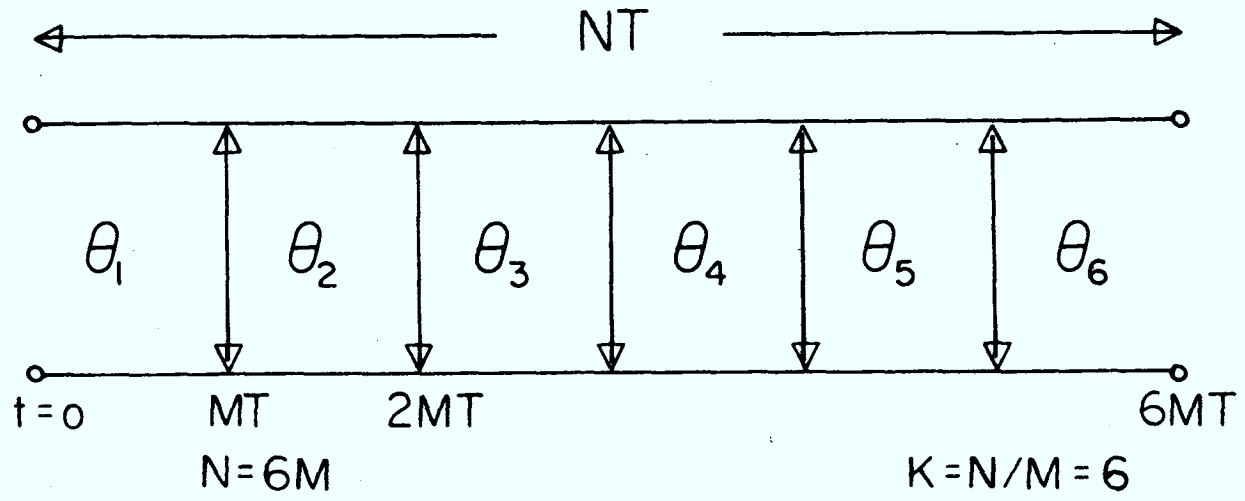

Figure 13 Model for a series of phase discontinuities.

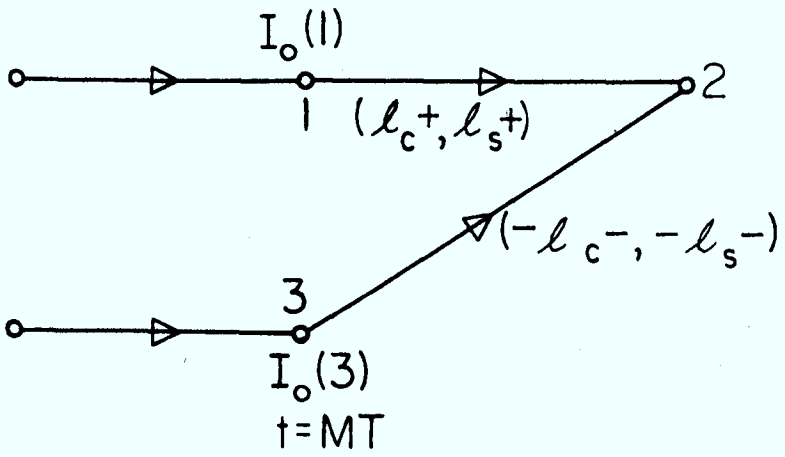

Figure 14 Illustration of the sequence detection algorithm at a phase jump.

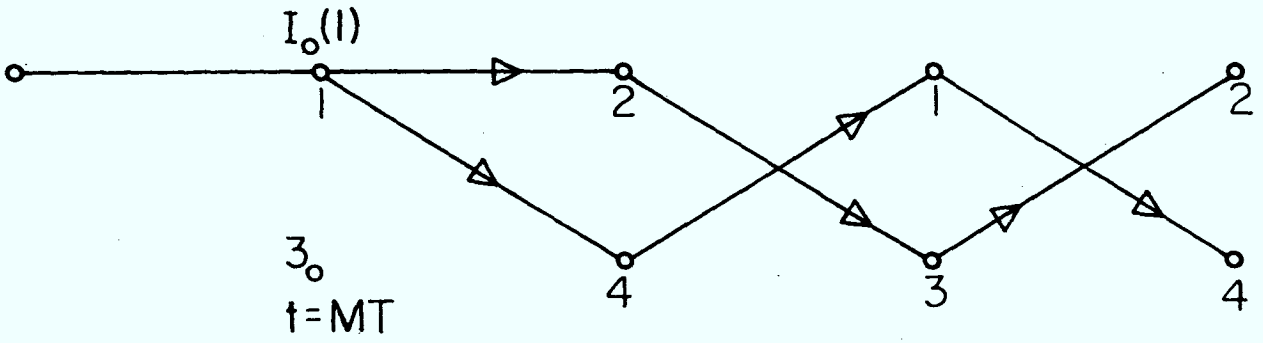

Figure 15 Illustration of the common factor I_o (1) at a merge in the modulation trellis.